MILITARY TECHNICAL COLLEGE
CAIRO - EGYPT

7th INTERNATIONAL CONF. ON
AEROSPACE SCIENCES &
AVIATION TECHNOLOGY

THE CHARACTERISTICS OF CYLINDRICAL WATER-COOLED FURNACES WHEN BURNING LIQUID, GASEOUS, OR DUAL LIQUID-GAS FUELS

A. RAZEK A. FATTAH *, M.A. NOSIER **, M.A. SHAHIEN *** and N.M. ALKADI ****

ABSTRACT

Measurements inside a flame tube are presented and compared for a range of confined liquid fuel oil, gaseous fuel and dual fuel flames. The operating conditions include a range of three heat inputs 29 kW, 38 kW and 48 kW. For dual fuel flames three gaseous fuel ratios 25 %, 50 % and 75 % are considered. The experimental work takes place using an industrial type, dual fuel burner that is especially designed and constructed to utilize the three types of firing. This burner is fitted to a water cooled cylindrical furnace (the Combustor).

It is found that, Burning gaseous fuel simultaneously with liquid fuel oil, acts as a hot shield surrounding the oil spray flame. This shield serves to reduce significantly the loss of combustibles from oil flames, mainly through enhancing the evaporation process of fuel oil droplets and increasing soot burnout at the flame region as well as preventing the surviving soot particles from being deposited on furnace walls. The importance of these conclusions emerges when burning low grade fuels or bituminous fuels which needs a more carefully designed combustion system.

KEY WORDS

Combustion, Liquid Fuel, Gaseous Fuel, Dual Fuel, Burners, Combustor Efficiency, Soot Emission.

* Professor of Mechanical Engineering, Helwan University. Cairo, Egypt. ** Associate Professor of Mechanical Engineering, Ain Shams University, Cairo, Egypt. ***Associate Professor of Mechanical Engineering, Helwan University, Cairo, Egypt. **** Mechanical Engineer, Organization for Energy Conservation and Planning, Cairo, Egypt.

NOMENCLATURE

AFH	Accumulative Fraction of Heat Transferred, (%)
C_{pw}	Specific Heat of Water Under Constant Pressure,(kJ/kg °C).
C.V.	Calorific Value of Fuel Used, (kJ/kg).
D_{in}	Combustor Inner Diameter (m).
FH	Fraction of Heat Transferred, (%)
HF(i)	Heat Flux to Segment i, kW/m^2.
L_i	Length of segment i (m).
$m_{c.w}$	Cooling Water Flow Rate, (kg/s).
m_F	Fuel Flow Rate, (kg/s).
n	No. of Combustor Segments.
R	Combustor inner radius (m).
S_i	Segment No. i
T_i	Inlet Temperature of Cooling Water, (°C).
T_o	Outlet Temperature of Cooling Water, (°C).

1. INTRODUCTION

The main concern in furnaces, boilers and gas turbines design is to obtain a stable flame, with high combustion efficiency and minimal noise and emission levels at a wide range of operating conditions. Such flame would allow for more energy savings and for lower environmental pollution.

The core of any combustion system is its burner. Continuous research and development work are carried out by the burners manufacturers in order to achieve the above aims. A large amount of information and research work are available for single fuel burners and multifuel burners which are designed to burn more than one type of fuel, but not simultaneously [1-20]. This is why sufficient information for simultaneous burning of more than one type of fuel, is scarce. With the increasing availability of Natural Gas in Egypt, emphasis has been placed on obtaining sufficient information for the effect of using gaseous fuel instead or along with the presently used liquid oils. Those information would contribute to a basic understanding of the structure and characteristics of dual fuel flames.

2. EQUIPMENT AND EXPERIMENTAL WORK

2.1 Test Rig Description

The experimental arrangement is shown in Fig. 1. It comprises the combustor which is a horizontal cylindrical water-cooled flame tube of 0.4 m inside diameter and 2.0 m long. Cooling is via water jacket which is divided into thirteen axial segments. Each segment

receives water at room temperature, and discharges it to drain. The Combustor is fitted with a coaxial dual fuel burner as illustrated in Fig. 1. The construction of the burner used is similar to those commonly used in large power stations and petroleum refineries in Egypt and probably elsewhere; (e.g. Abou-Sultan power station). It is a double-swirl type: the two swirlers are concentric as shown in Fig. 2. In this arrangement, a liquid fuel oil is sprayed by a 60° swirl atomizer placed at the center of the primary (inner) air swirler of 45° vane angle. Four identical holes were opened through the vanes of the outer secondary air swirler of 30° vane angle to allow for the fixation of four identical gaseous fuel burners. These gaseous burners are placed off-axis of combustor, and distributed at equal circumferential distance along a circle having a diameter of 0.136 m. Hence they are mounted at the ends of two perpendicular diameters of that circle as shown in Fig. 2 Combustion air is supplied to the burner by an electric air blower. The air flow rate is measured by a standard, calibrated orifice plate connected to a U-tube water manometer The liquid fuel used is gas oil (solar) with an approximate weight analysis of 86.3 % C 12.8% H_2, 0.90% S. The average heating value and density are 44162 kJ/kg, 820 kg/m^3 respectively. The liquid fuel mass flow rate is measured by means of pressure gauge indicator which is calibrated to read the mass flow rate. The gaseous fuel used is a commercial LPG fuel with a volumetric approximate analysis of 70% (C_4 H_{10}) and 30% (C_3 H_8) and an average heating value of 47092 kJ/kg. The gaseous fuel mass flow rate through each gas burner is measured by means of a calibrated orifice meter.

In the present work, average flame temperature is measured using a fine-wire thermocouple, water-cooled probe. The basic design has been previously used by many investigators [7,10]. The thermocouple is made of Platinum and 10% Rhodium-Platinum wires of 100 μm diameter and connected to an electronic integrator and a millivolt- meter The soot concentration is measured using the well known Bacharach tester. The heat flux to the combustor walls is measured through the measurements of the specific enthalpy rise and the flow rate of cooling water in each segment. The enthalpy rise is calculated by measuring the cooling water temperature difference between outlet and inlet. The cooling water flow rate in each segment is determined by collecting a certain volume of the outlet water and measuring the corresponding time [18]. Provisions were made to check the flow rate through each segment at least two times for each run. The outlet water temperature at each segment was measured by type E thermocouple (Nickel Chromium - Copper Nickel) which is located at the segment exit. The values of temperature are displayed on digital thermometer having a resolution of 0.1°C. The heat flux to each segment is calculated using the simple formula :

$$HF_{in} = \frac{[\dot{m}_w \times C_{pw} \times (T_o - T_i)]_{in}}{(\Pi \times D_{in} \times L_i)} \qquad (1)$$

2.2 Experimental Procedure.

The aim of the experimental procedure is to investigate and to compare both the flame structure and the characteristics of the combustor under three types of firing. These types of firing are :

1. Liquid fuel firing.
2. Gaseous fuel firing.
3. Dual (simultaneous) fuel firing.

A range of three heat inputs are included in each firing type. These chosen three heat inputs are 29 kW, 38 kW and 48 kW with an excess air factor of 20% which is kept constant during the groups of test runs. Also, for the dual fuel firing where liquid fuel and gaseous fuel are fired simultaneously, three gaseous fuel ratios are chosen namely; 25%, 50% and 75%. Accordingly, a total of 15 test runs are carried out. The operating conditions for these runs are shown in table 1, whereas Fig. 3 exhibits photographs for the corresponding flames .

3. DISCUSSION OF RESULTS

3.1 Liquid Fuel Oil Flame Structure.

The experimental results obtained for the three oil flames of runs 1,2 and 3 together with visual observations, allowed the formulation of a physical description of the flame structure common to the three flames. The liquid fuel oil leaves the atomizer in the form of a hollow conical spray with a central air core. The swirled combustion air creates a recirculation zone which surrounds the fuel atomizer, as also observed previously, e.g. Chigier[25]. The spray sheet travels through this reverse flow zone and as a result, small droplets and fuel vapour are recirculated inside this zone. In addition, the presence of this recirculation zone displaces droplets found near the centerline towards the outer edge of the spray. This results in a transportation of a number of droplets outside the nominal spray boundary, Presser et al.[1]. Across the shear layer, which encloses the recirculation zone, the high turbulent mixing rates and the comparatively high temperature of the recirculated gas allowed chemical reaction to proceed with a high intensity. This region extends to the fuel spray region and there, the resulting high temperature increases the droplets evaporation and helps to stabilize the flame. The radial profiles of temperature for the three oil flames of runs 1,2 and 3 are shown in Fig. 4. Although the temperature profiles for the three oil flames indicate the same general trend, quantitative differences exist in the temperature values and in the relative dimensions of the central high intensity combustion, high temperature zone. The temperature increases appreciably across the flame boundaries e.g. at axial location of x/D=0.125 and r/R=0.2. Far downstream locations, at x/D >0.625, the combustor is fully occupied with non-luminous combustion gases and the temperature levels exhibit gradual decline along the combustor down-stream direction due to convective heat transfer to the cooling jacket. The shape of these profiles tends to even-out due to turbulent diffusion effects. The final concentration of soot at exit

is expected to be determined by the combined effects of formation and burnout, which are influenced by the temperature throughout the flame [14]. In general, high temperature levels lead to lower soot concentration. It is clear, therefore, that the values of temperature and soot concentration are different when comparing the three oil flames of runs 1,2 and 3. These differences may be attributed to the spray quality of each flame which indirectly affects the temperature field. The droplet size which is greatly affected by the fuel atomization pressure plays a major role in the combustion performance of spray flames, Chigier[25]. The three flames correspond to three atomizing pressures namely; 3.5, 7.5, 12 bars. For the flame of run 1, the slow evaporation of its comparatively large droplets provides a small amount of fuel vapor at the spray region and, therefore, the dilution and quenching of chemical reaction effects of the surrounding air stream will result in a reduction in the combustion intensity. This is supported by the relatively low temperature values measured along the combustor. In addition, it is also confirmed by the relatively high accumulation rates of condensed fuel vapor experienced in the sampling system during soot concentration measurements. For the flames of runs 2 and 3 which are characterized by higher atomization pressures, larger number of finer droplets and hence faster evaporation rate is experienced. Accordingly, an intense chemical reaction will be ensured, leading to elevated temperature levels. This is evident by referring to Figs. 4(b,c) which show a higher temperature values compared to the oil flame of run 1 shown in Fig. (4.a).

3.2 Gaseous Fuel Flame Structure.

The flames of the gas burners used are partially premixed, by virtue of the existing ports of the burner tube. The fuel/air mixture issuing from the burner entrains secondary air from the combustor space, intermingle with it, and burns intensely with a blue-coloured flames , see Fig. 3. Such premixing results in a single peak of temperature that coincides nearly on gas burner centerline, which is strictly true at close distances from gas burner exit. This is clear in Fig. 5 (a,b,c) where the maximum temperature occurs at r/R=0.30 and x/D=0.125. At further downstream locations, temperature values tend to fall off, and even out across the combustor flow cross-section, mainly due to heat transfer to walls and gas mixing, augmented by swirl motion. The level of soot for the gaseous flames is found negligible, which indicates the clean combustion pattern of gaseous flames.

3.3 Dual Fuel Flame Structure.

a. Gaseous Fuel Ratio 25%.

For such low gas fuel ratio (runs 7,8,9) the gaseous four flames are too small to significantly interact with the oil flame, refer to Fig. 3. However, the existence of gaseous flames around the oil flame seems to improve , somehow, the evaporation of some fuel oil droplets in the near region of gas burners. This is consistent with the reduction in soot levels at combustor exit in this case, as shown in Fig. 6, compared with the corresponding levels of pure fuel oil flames. Close inspection to these figures suggests that the basic dual

fuel flame structure has a combined features of both oil flames and gaseous flames. As shown in Fig. 6, , two peak temperature values are recorded at x/D = 0.125, r/R = 0.15 and 0.35. The first peak corresponds to the oil flame whereas the second to the gaseous flame. The spreading of the oil flame seems to be slightly reduced at x/D = 0.375 compared to the cases of pure oil flames, compared with Fig. 4. This is attributed to the existence of the four gaseous flames that contributes, in this case, to some extent in rectifying the oil flame.

b. Gaseous Fuel Ratio 50%.

The radial temperature at different axial locations are shown in Fig. 7 for the flames having gaseous fuel ratio of 50% which correspond to runs 10,11,12. During these runs, gaseous fuel flow rates are increased whereas liquid fuel oil rates are decreased while maintaining the same fixed three heat inputs mentioned above. Although the reduction in fuel oil rates was accompanied by a corresponding reduction in fuel oil atomizing pressure, the existence of the four gaseous flames seem to compensate the drawback of this by modifying the evaporation characteristics of the fuel oil droplets. It is also observed that the soot concentrations at the exhaust port of the combustor during these runs are lower than those of the cases of 25% gas-fuel ratio (runs 7,8 and 9).

c. Gaseous Fuel Ratio 75%.

Under this high value of gaseous fuel rates, (runs 13-15), great interaction seems to occur between the oil flame and the gaseous flames. The colour of the oil flame is converted from a dark luminous flame to a bright luminous one characterised by lower levels of soot formation and higher levels of temperature compared to runs (1-3 and 7-12) which relate to cases of lower gaseous ratio. In addition, the existence of this intense interaction between the flames greatly contributes in shortening the oil flame length via accelerating evaporation of oil droplets. Fig. 8 illustrates the radial profiles of temperature. In comparison with the case of less gaseous fuel ratio, it is observed that the region of interaction between gaseous flames and fuel oil flames is further extended to cover more space in the fuel oil flame. The gaseous fuel flame seems to survive up to x/D = 0.375 , manifested by the single peak temperature whereas the oil flame peak temperature is almost vanished.

3.4 Heat Flux Distribution to The Combustor Walls.

Fig. 9(a,b,c) shows the heat flux distribution to the combustor walls at different heat inputs and under different types of firing. As a common feature, heat flux peaks at about x/D=0.250, where this region is characterized by an intense chemical reaction as well as favourite radiation characteristics. The effect of varying the heat input on the peak heat flux was found to die down as the gaseous fuel ratio increased. For example for pure oil-fuel flame, it was found that increasing the heat input from 29 to 48 kW would increase the peak heat flux by a factor of 2.28. On the other hand this same factor is reduced to 1.71 for the flame of 75% gaseous fuel ratio, and reduced even further to only 1.57 for

the pure gaseous-fuel flame. This indicates that using gaseous fuel simultaneously with a liquid-fuel flame would cause the heat flux peak value to be less sensitive to variations in heat input to the combustor (i.e. versus variable load operation of the combustor). This may be attributed to the sensitivity of the atomization process of oil flames under variable load. A process whose effect is overshadowed when gaseous flames coexist with oil flames.

3.5 The Accumulative Heat Transferred to The Walls.

The accumulative heat transferred to the combustor walls equals the sum of the heat transferred to all segments of the wall. For any segment , for example no.(i) , the fraction of heat transferred to it is given by :

$$FH(i) = \frac{[m_{w} \times Cp_{w} \times (T_{e} - T_{in})](i)}{(m_{f} \times C.V.)} \times 100\% \qquad (2)$$

The accumulative fraction of heat transferred that is given off by the flame up to segment no.(n) is given by :

$$(AFH)(n) = \sum_{i=1}^{i=n} FH(i) \qquad (3)$$

If 'n' in this equation designates the last segment of the wall, (AFH) value would equal the total fraction of heat transferred to the combustor wall , i.e. equals the thermal efficiency of the combustor [17,22].

As shown in Figs. 10(a,b,c) for a fixed heat input, increasing the gaseous fuel ratio greatly increases the accumulated heat transferred. This result directly reflects a favourite effect of introducing gaseous flames together with oil flames. This is mainly due to the contribution of gaseous flames in enhancing the evaporation and combustion characteristics of oil flames specially at poor atomizing conditions which is likely to ensue, for example, at low oil fuel percentage..

3.6 Thermal Efficiency of The Combustor and Soot Concentration at Exhaust Port

Figs. 11 and 12 show comprehensive comparisons of the combustor characteristics under different types of fuel admitted and at different heat inputs. Fig. 11 shows the effect of gaseous ratio and heat input on thermal efficiency while Fig. 12 presents the effect of the same two variables on soot levels at combustor exit. These figures indicate that thermal efficiency of the combustor can be raised and soot emission levels reduced by means of the following two actions:

a) increasing the gaseous fuel ratio ; or

b) increasing the heat input.

4. CONCLUSIONS

From observations and analysis of the experimental results, the following main conclusions may be summarized as follows :

1. Adoption of the gas flame jets, placed around the central oil flame, assisted by the swirling motion of air, acts as a hot jacket to the oil flame. This jacket reduces significantly the loss of combustibles from the oil flame, presumably through evaporating and burning the falling and flying oil droplets and soot particles

2. For a fixed heat input, increasing the gaseous fuel ratio, has the following advantages:
   (a) Faster attainment of uniform radial distribution of temperature which augments the convective heat transfer rates.
   (b) Obtaining more uniform heat flux along the combustor downstream direction.
   (c) Increasing the accumulative heat transfer to the combustor walls, and consequently raising the thermal efficiency.
   (d) Reducing the soot concentration levels at combustor exit.
   (e) Less sensitivity of the peak value of the heat flux to variations of heat input (i.e. versus variable load of the combustor)

3. For the three types of firing examined, under the volume and configuration of the present combustor, an increase in loading(heat input) within the tested range (29-48 kW), causes an increase in both heat flux intensity and thermal efficiency.

4. The adoption of dual fuel firing makes it easy to control heat transfer mode and stream-wise distribution of heat flux. Thus dual firing with low gas ratio should be adopted for a principal radiative-heat-transfer-mode with a peak at the region close to the burner end. On the other hand dual firing with high gaseous fuel ratio may be used for a process that is dependent on convective heat transfer mode with a rather more uniform heat flux distribution.

REFERENCES

1. Presser,C., Gupta,A.K. and Semerjian,H.g., "Droplet Transport in a Swirl-Stabilized Spray Flames," The eighth International Conference for Mechanical Power Engineering, Alexandria University, Alexandria, Egypt, April, 1993.

2. El-Mahallawy,F.M., Farag,S.A. and Yowakim, F.M.," Effect of Some Parameters on the Radiant Heat transfer in a Cylindrical Oil-Fired Furnace," First Conference of Mechanical Power Engineering, Cairo University, Cairo, Egypt, Feb. 1977.

3. El-Mahallawy,F.M., Khalil,E.E and Abdel Aal O., "Characteristics of Water Cooled Flame Tube," Fourth International Conference for Mechanical Power Engineering, Oct., Cairo, Egypt, 1982.

4. Moneib, H.A., Ismail, M.A., and Hussien, A.M.," Characteristics of Swirling Oil Flames in a Cylindrical Furnace with Variable Quarl Geometry," 7th International Conference of Mechanical Power Engineering, Cairo University, Vol. II , Dec. 1990.

5. El-Mahallawy,F.M., Hassan,M.A. and Eid, M. H., "Influence of Firing Parameters on Oil Fuel Combustion in Flame Tubes," The Eighth International Conference for Mechanical Power Engineering, Alexandria University, Alexandria, Egypt, April, 27-29, 1993.

6. El-Banhawy,Y.H.,Elehwany,A.A. and Hagag,E.a.,"The Combustion Characteristics of Swirl/Disc-Stabilized Spray Flames," Seventh International Conference of Mechanical Power Engineering, Cairo University, 1990.

7. El-Mahallawy,F.M., Mahdi Ali,E. and Rashad, "Characteristics of Combustion Heat Liberated Down Stream of Circular Bluff Bodies," Proceeding of Second Conference of Mechanical Power Engineering, Vol.2, 1978, Cairo, PP. 1-12.

8. El-Banhawy,Y.H., and Whitelaw,J.H.," Experimental Study of The Interaction Between a Fuel Spray and Surrounding Combustion Air," Combustion and Flame, Vol.42, 1981, PP.253-275.

9. El-Banhawy,Y.H., " Open and Confined Spray Flames," Ph.D.Thesis, University of London, England, 1980.

10. Elghoroury,S. Abdullah," Effect of Stabilizing Cone Angle and Swirling Action on Confined Flame structure," Ph.D, Thesis, Cairo University,1990.

11. Wu, H.L. and Fricker, N.,"The characteristics of Swirl Stabilized Natural Gas Flames," Journal of the Institute of Fuel , 1976 PP. 144-151.

12. Yuasa, S., "Effect of Swirl on the Stability of Jet Diffusion Flames," Combustion and Flame Journal, Vol.66, PP. 181- 192, 1986,.

13. El-Mahallawy, F.M., and Abbas, A.S.," Effect of Swirling of Fuel and Air Streams of Heat Liberation in Cylindrical Gas Furnace," Bulletin of the Faculty of Engineering, Cairo University, 1978.

14. Nishida,Osami and Mukohara,seiya," Characteristics of Soot Formation and Decomposition in Turbulent diffusion Flames," Combustion and Flame, Vol. 47, 1982, PP 269-279.

15. Adel Salam,M.S.," Heat Transfer in Cylindrical Flame Tubes," Proceeding of second conference of Mechanical Power Engineering, Cairo, September, 1978.

16. El-Mahallawy, F.M., Ali,E.Mahdy, Negm,S.M. and Rafat,N.M.," An Experimental Investigation of The Effect of Exit Section Geometry and Furnace Length on Heat Liberation in a Cylindrical Gas Fired Model Furnace," Proceeding of second Conference of Mechanical Power Engineering, Cairo, September, 1978.

17. H.L., WU. "Comparison of the Performance of Natural Gas and Oil Flames in a Cylindrical Furnace," Journal of the Institute of Fuel, pp 316-323, August, 1969.

18. Barakat, H.Z. and Gad EL-Mawla. "Study of the Performance of Radiant Type Furnace When Firing Gaseous and Liquid-Gas Fuel,." Second Conference of Mechanical Power Engineering, Cairo, September, 1978.

19. Sabry, T.I., Elaskary, A.H., Sheta, M.M. and Mohamed,E.A., " Theoretical Analysis on Heat Transfer From Diffusion Flames with Gaseous Fuel Injection," The Eighth International Conference for Mechanical Power Engineering, Alexandria University, Alexandria, Egypt, April 27-29, 1993.

20. Ibrahim Said, M.A., Moneib, H.A. and Waley, M., " Structure and Radiative Properties of Pulverized Coal/Gas/Air Jet Flames," Seventh International Conference of Mechanical Power Engineering, Cairo University, 1990.

21. Chigier, N., "Optical Imaging of Sprays," Progress of Energy and Combustion Science, Vol. 17, PP 211-262, 1991.

Table 1

Operating Conditions of The Experimental Program.

Run No.	Fuel Type	Gaseous Fuel Ratio	Heat Input	$\dot{m}$ fuelx10^4	$\dot{m}$ airx10^2	Fuel Oil Pressure	Excess Air	A/F	Equivalence Ratio	Measurements of :
		%	(kW)	kg/s	kg/s	kp/cm2	%		(ϕ)	
1	Fuel Oil (Sular)	0	29	6.56	1.13	3.5	20	17.15	0.833	- Time average temperature.
2	Fuel Oil (Sular)	0	38	8.69	1.49	7.5	20	17.15	0.833	- Soot concentration.
3	Fuel Oil (Sular)	0	48	10.89	1.87	12	20	17.15	0.833	- Heat flux to the Walls.
4	Gaseous Fuel (LPG)	100	29	5.72	1.06	-	20	18.48	0.833	- Time average temperature.
5	Gaseous Fuel (LPG)	100	38	7.54	1.39	-	20	18.48	0.833	- Soot concentration.
6	Gaseous Fuel (LPG)	100	48	9.45	1.75	-	20	18.48	0.833	- Heat flux to the Walls.
7	Dual Fuel	25	29	6.39	1.12	2.1	20	17.48	0.833	- Time average temperature.
8	Dual fuel	25	38	8.41	1.47	3.5	20	17.48	0.833	- Soot concentration.
9	Dual fuel	25	48	10.53	1.84	6.2	20	17.48	0.833	- Heat flux to the Walls.
10	Dual fuel	50	29	6.17	1.10	1.7	20	17.81	0.833	- Time average temperature.
11	Dual fuel	50	38	8.22	1.46	2.1	20	17.81	0.833	- Soot concentration.
12	Dual fuel	50	48	10.17	1.81	2.5	20	17.81	0.833	- Heat flux to the Walls.
13	Dual fuel	75	29	5.95	1.08	1	20	18.15	0.833	- Time average temperature.
14	Dual fuel	75	38	7.83	1.42	1.25	20	18.15	0.833	- Soot concentration.
15	Dual fuel	75	48	9.81	1.78	1.4	20	18.15	0.833	- Heat flux to the Walls.

$\dot{m}$ (fuel) = Fuel mass flow rate (kg/s)

$\dot{m}$ (air) = Air mass flow rate (kg/s)

Gaseous fuel ratio = Percent gaseous fuel in flame.

$$= \frac{[\text{Gaseous Fuel Heat Input}]}{(\text{Total Heat Input})} \times 100\%$$

$$\phi = \frac{(F/A)_{(\text{Actual})}}{(F/A)_{(\text{Stoichiometric})}}$$

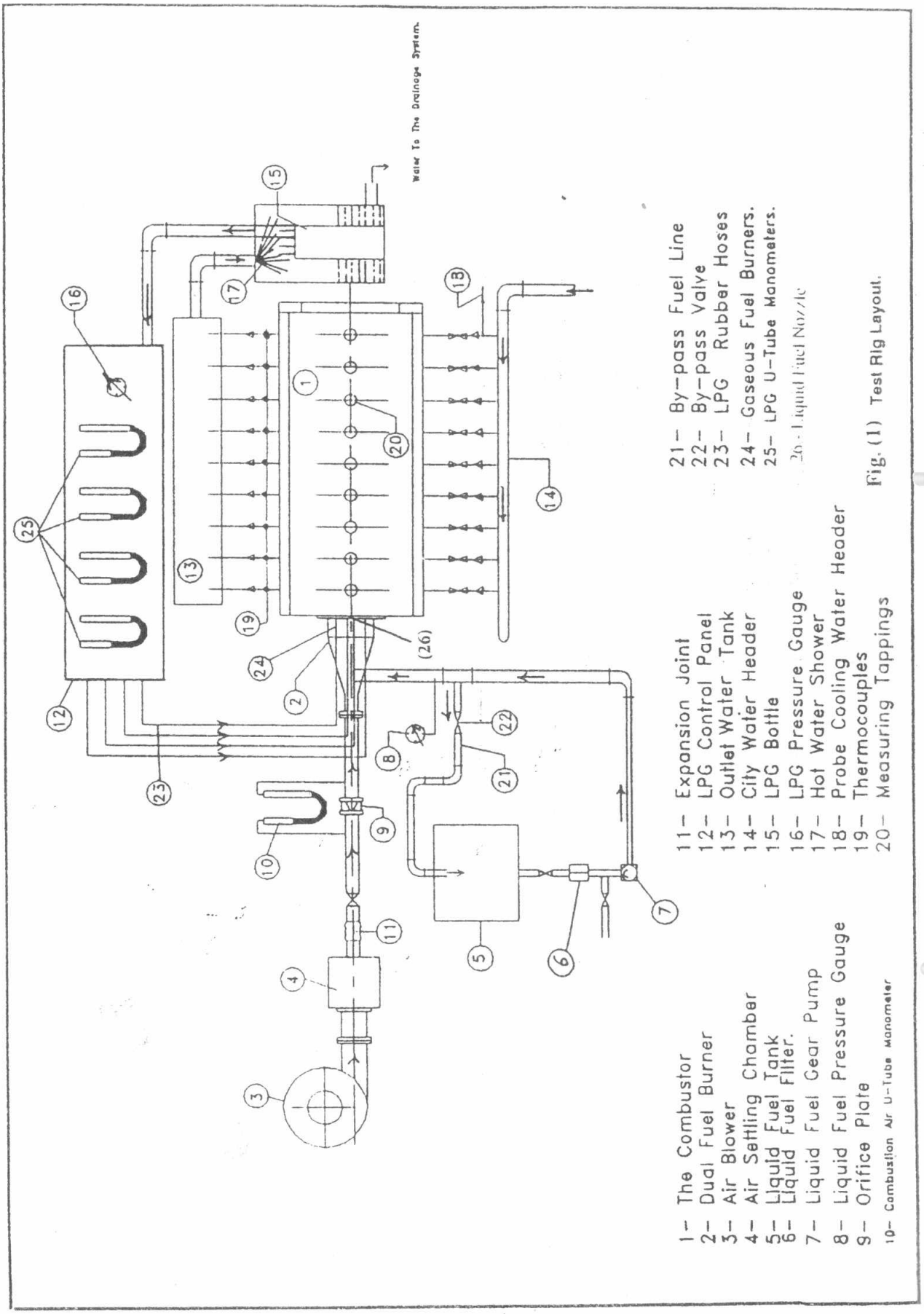

Fig. (1) Test Rig Layout.

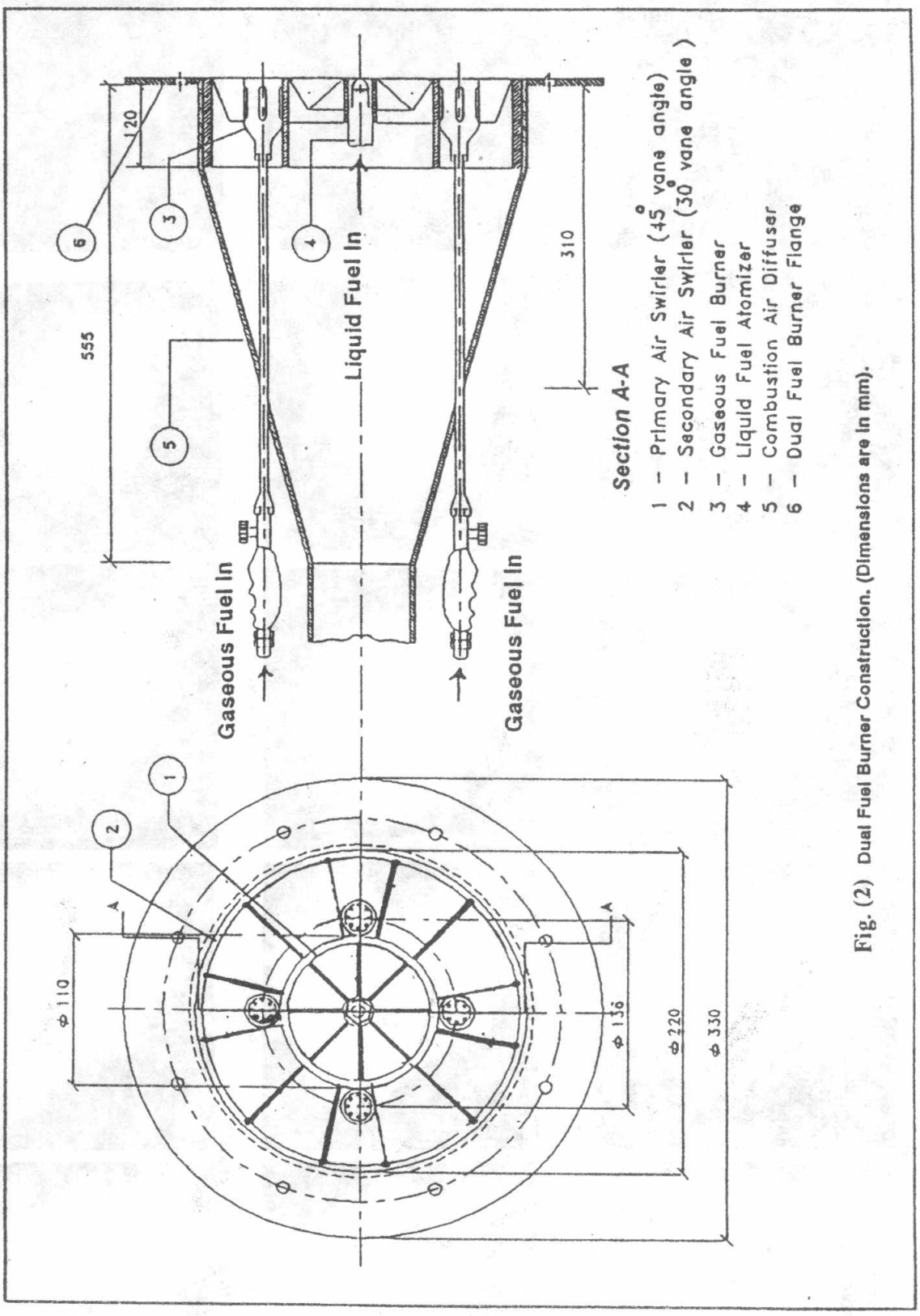

Fig. (2) Dual Fuel Burner Construction. (Dimensions are in mm).

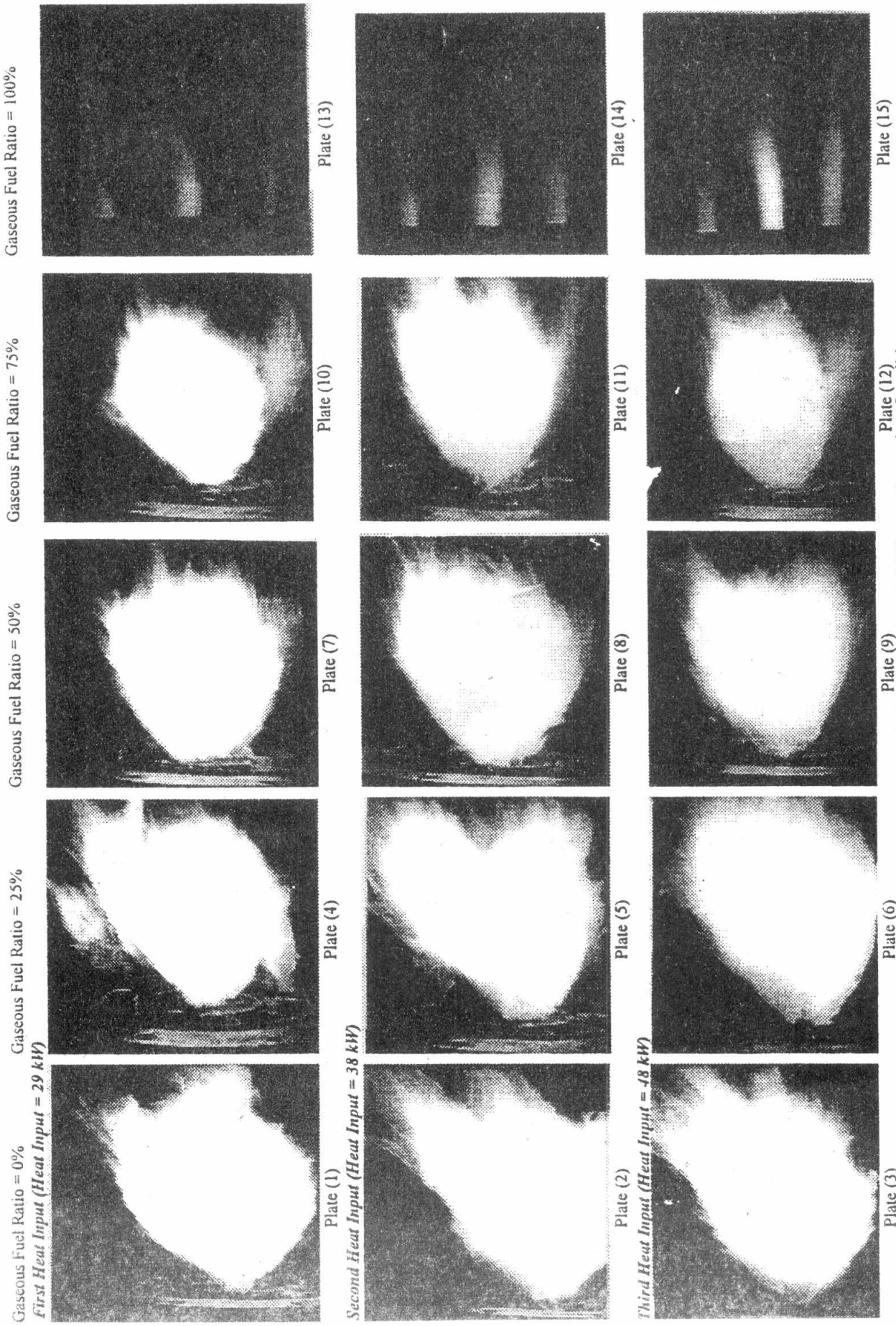

Fig. 3: Photographic Comparison Of The 15 Flames At Different Operating Conditions

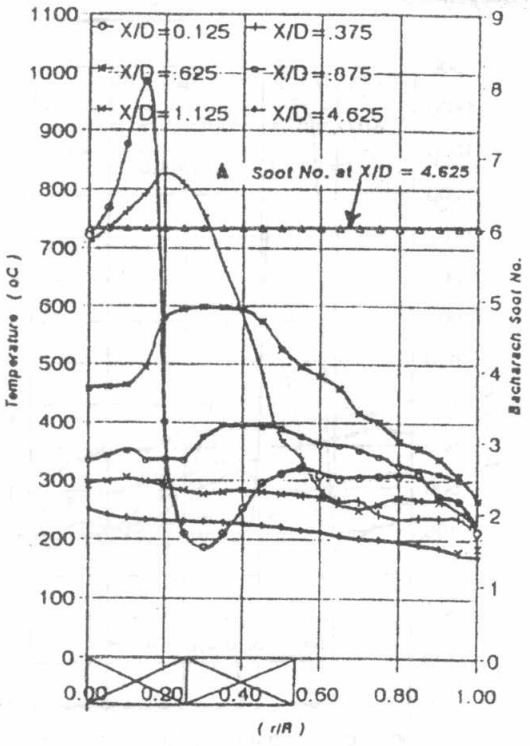

(a) - Run 1

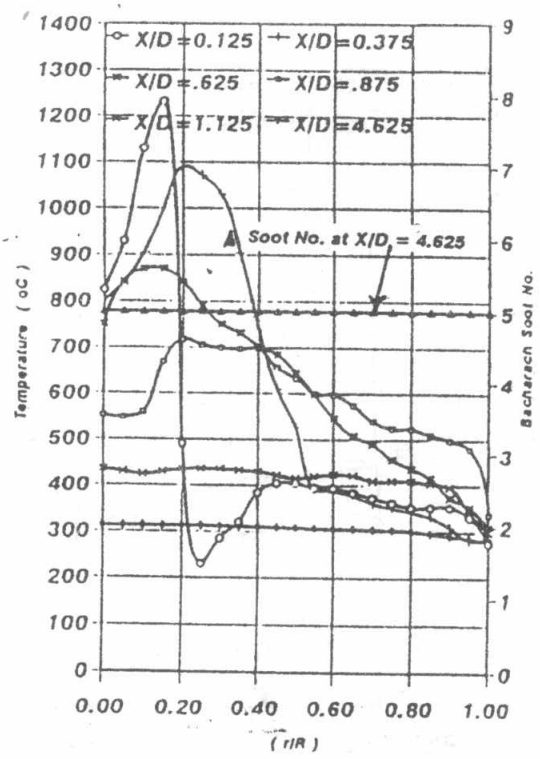

(b) - Run 2

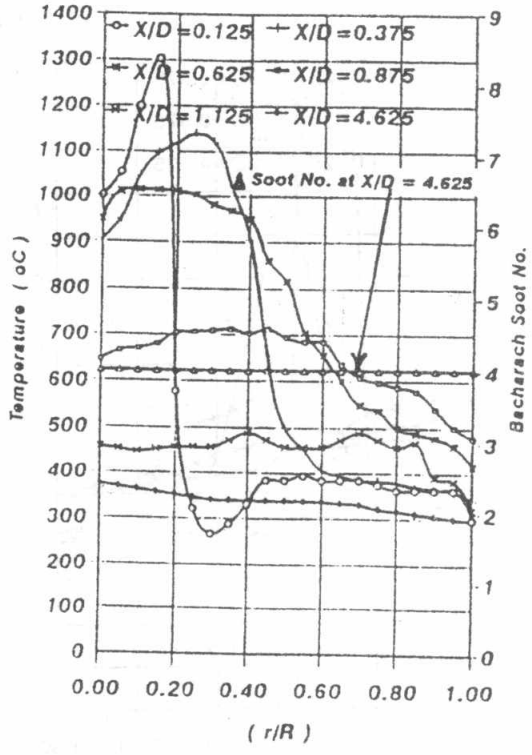

(c) - Run 3

Fig. 4 Radial Profiles of Temperature at Different Axial Locations and Soot Concentration at Combustor Exit - Runs 1,2,3.
Fuel Type : Fuel Oil (Solar)- Gaseous Fuel Ratio = 0 % - Equivalence Ratio(ϕ) -0.833
(a) Heat Input = 29 kW
(b) Heat Input = 38 kW
(c) Heat Input = 48 kW

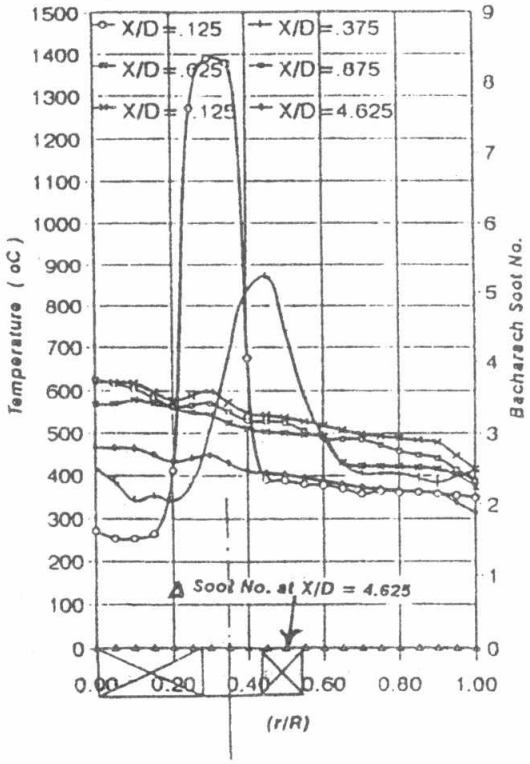

(a) - Run 4

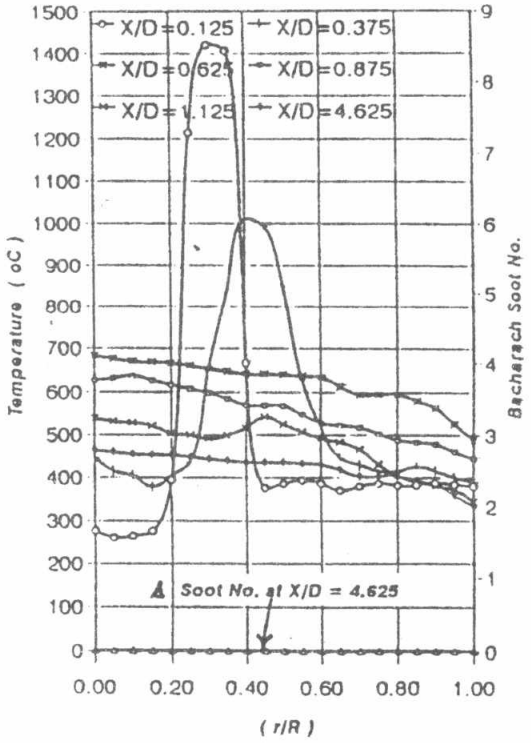

(b) - Run 5

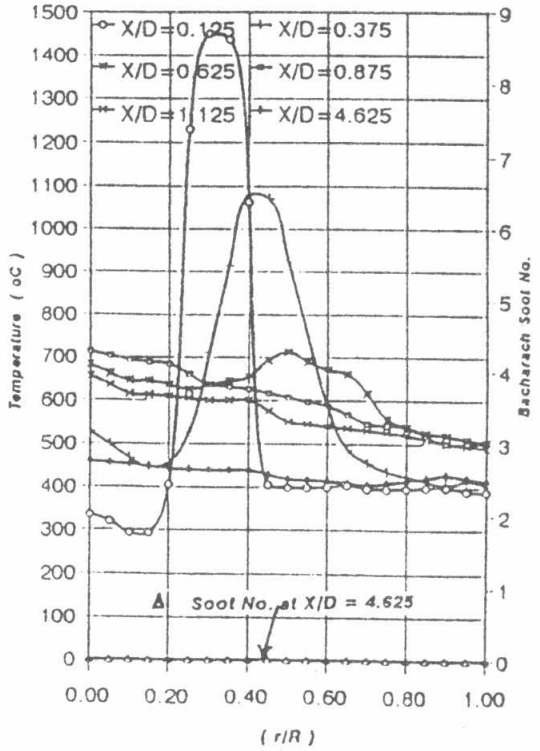

(c) - Run 6

Fig. 5 Radial Profiles of Temperature at Different Axial Locations and Soot Concentration at Combustor Exit - Runs 4,5,6.
Fuel Type : Gaseous Fuel (LPG) - Gaseous Fuel Ratio = 100 % - Equivalence Ratio(ϕ) -0.833
(a) Heat Input = 29 kW
(b) Heat Input = 38 kW
(c) Heat Input = 48 kW

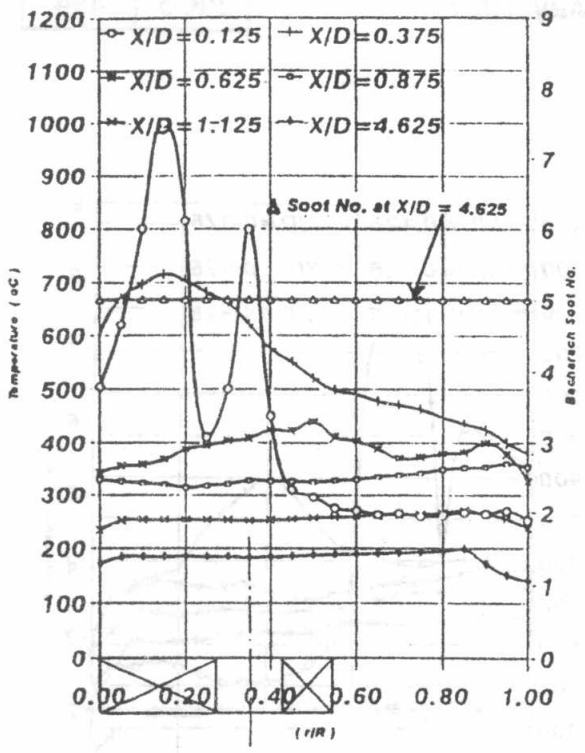

(a) - Run 7

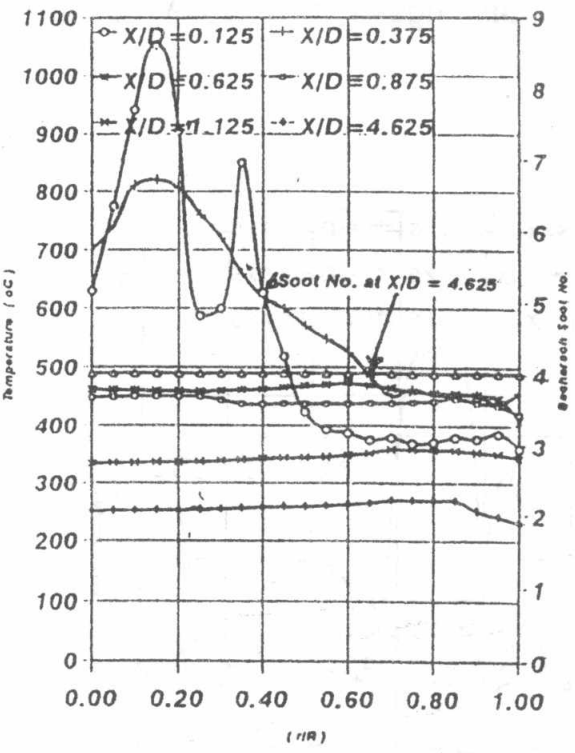

(b) - Run 8

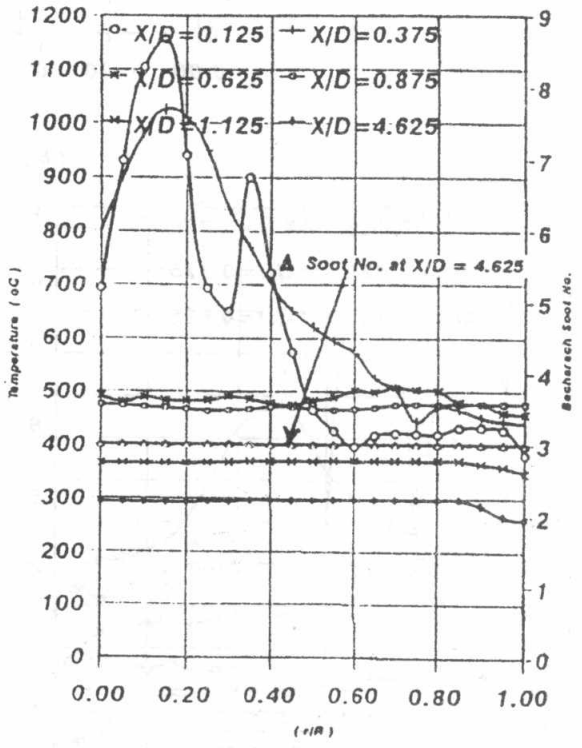

(c) - Run 9

Fig. 6 Radial Profiles of Temperature at Different Axial Locations and Soot Concentration at Combustor Exit - Runs 7,8,9.
Fuel Type : Dual Fuel - Gaseous Fuel Ratio = 25 % - *Equivalence Ratio* (ϕ) -0.833
(a) Heat Input = 29 kW
(b) Heat Input = 38 kW
(c) Heat Input = 48 kW

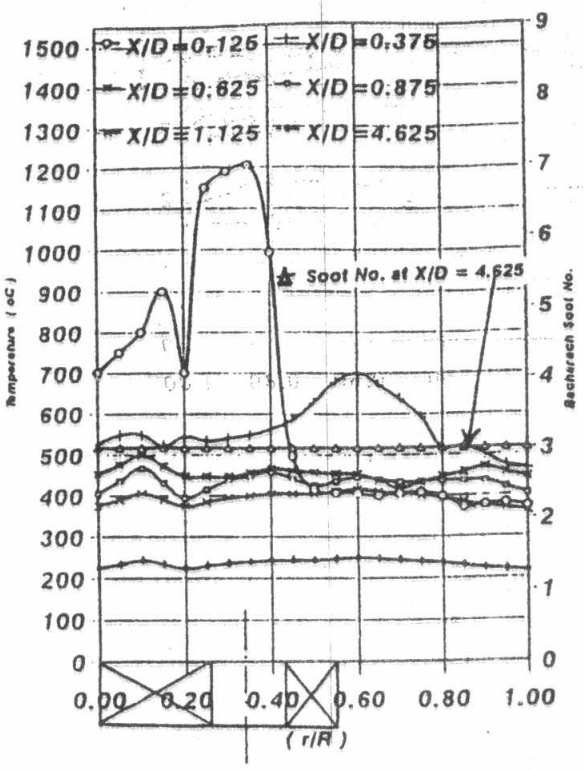

(a) - Run 10

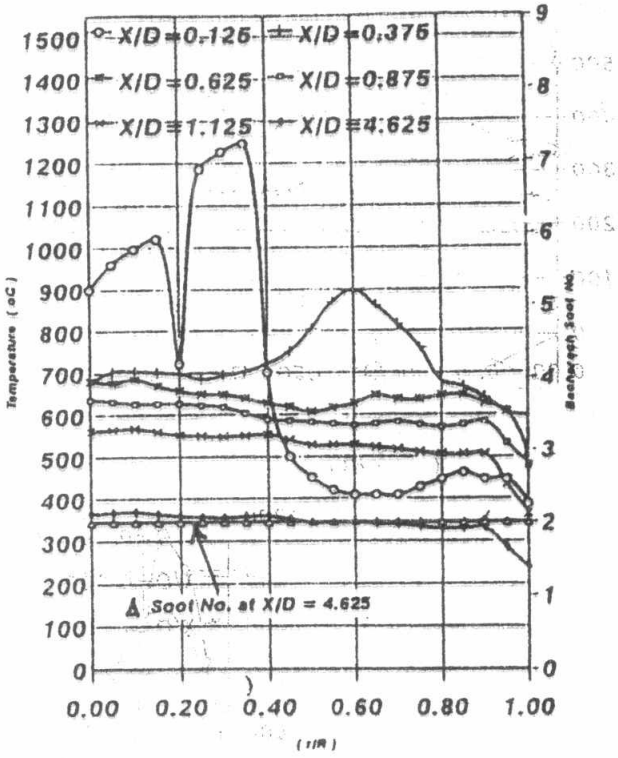

(b) - Run 11

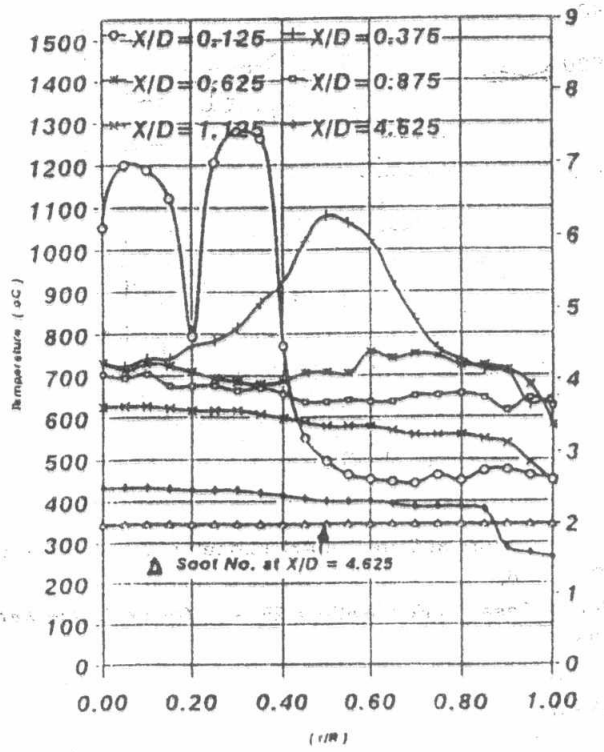

(c) - Run 12

Fig. 7 Radial Profiles of Temperature at Different Axial Locations and Soot Concentration at Combustor Exit - Runs 10,11,12.
Fuel Type : Dual Fuel - Gaseous Fuel Ratio = 50 % - *Equivalence Ratio*(ϕ) -0.833
(a) Heat Input = 29 kW
(b) Heat Input = 38 kW

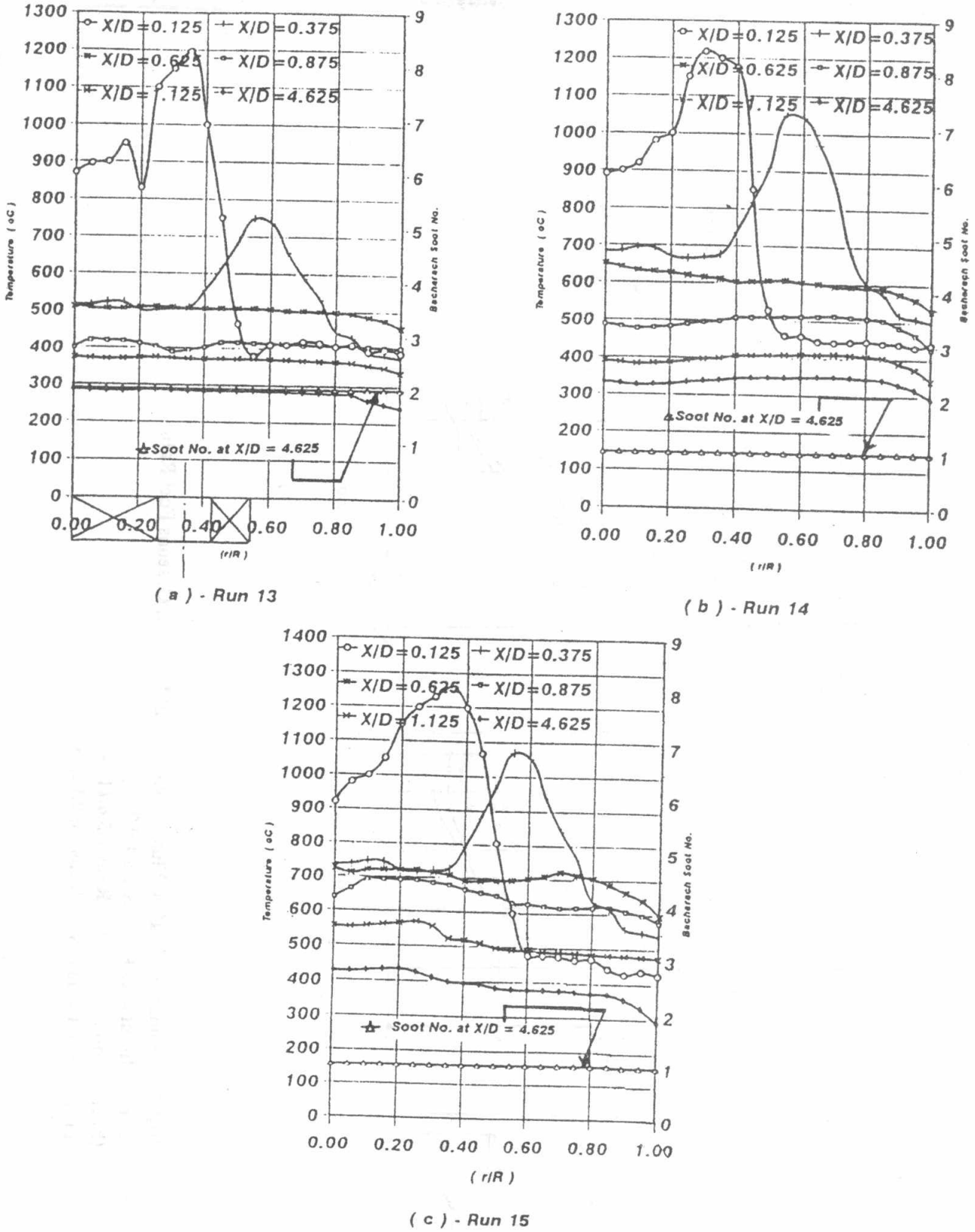

Fig. 8 Radial Profiles of Temperature at Different Axial Locations and Soot Concentration at Combustor Exit - Runs 13,14,15.

Fuel Type : Dual Fuel - Gaseous Fuel Ratio = 75 % - *Equivalence Ratio* (ϕ) = 0.833

(a) Heat Input = 29 kW

(b) Heat Input = 38 kW

(c) Heat Input = 48 kW

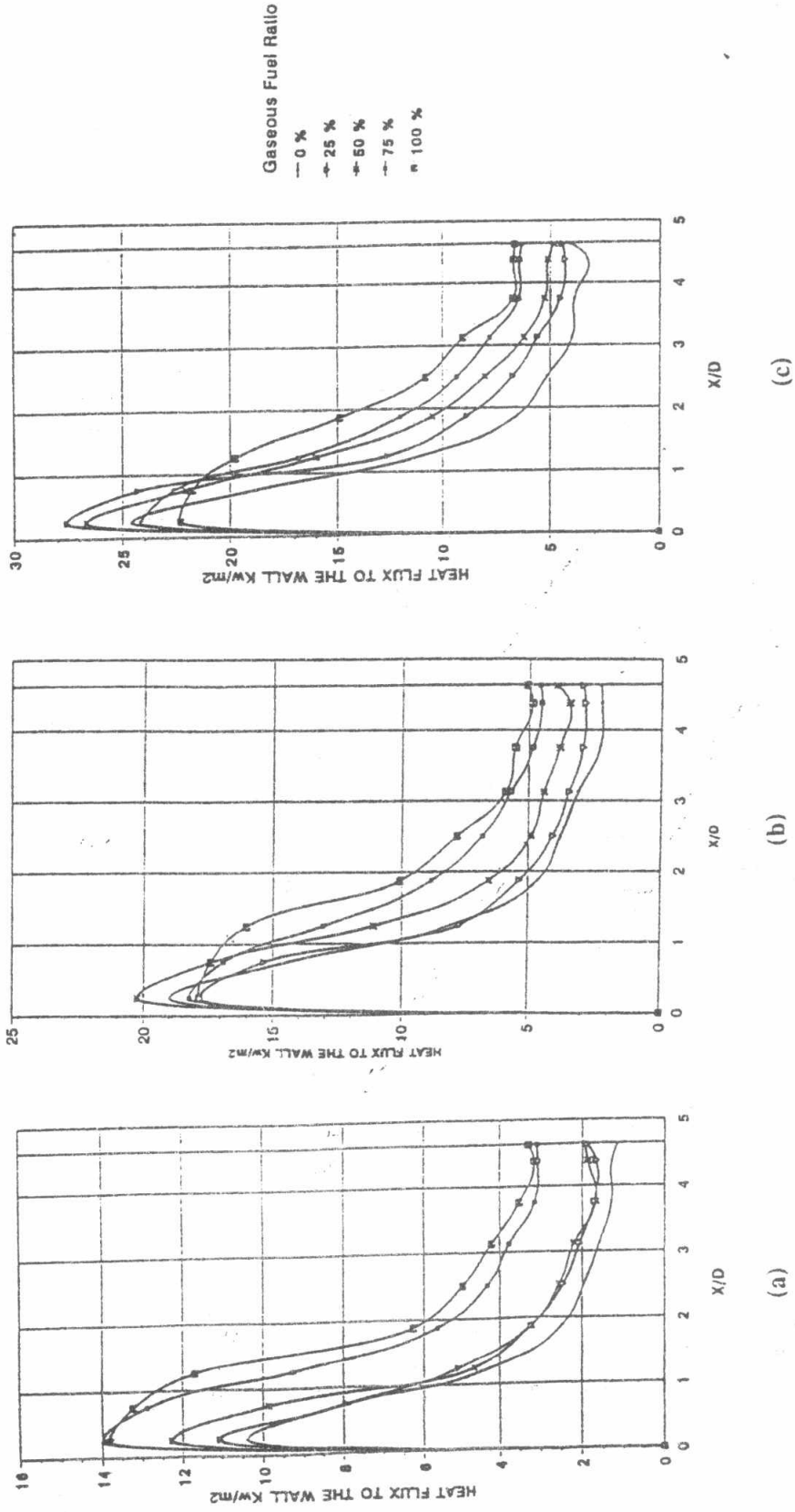

Fig. 9 Comparison of Heat Flux Distribution at Different Gaseous Fuel Ratios.
(a) Heat Input = 29 kW Runs 1,4,7,10,13
(b) Heat Input = 38 kW Runs 2,5,8,11,14
(c) Heat Input = 48 kW Runs 3,6,9,12,15

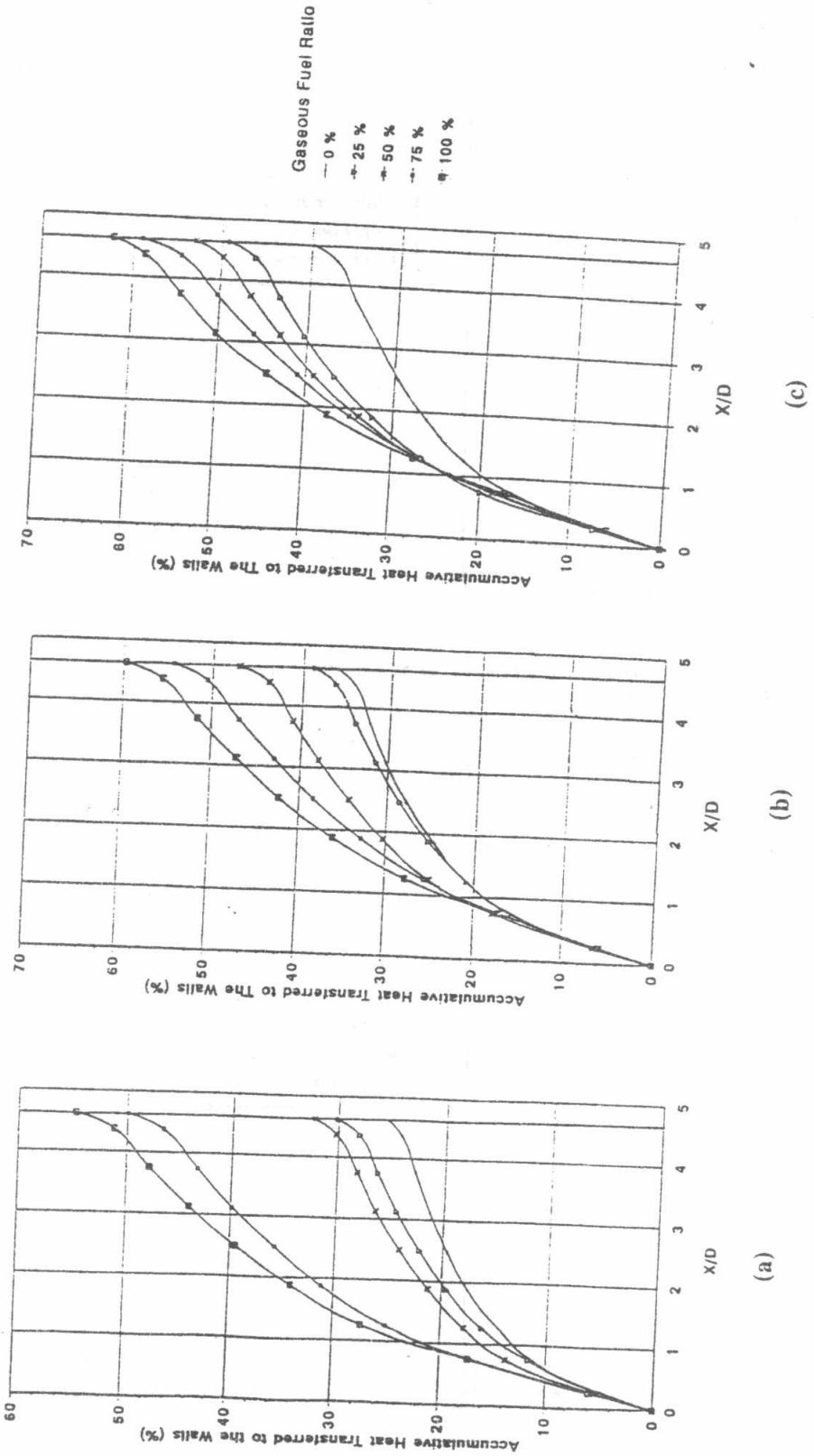

Fig. 10 Comparison of Accumulative Heat Transfer to The Combustor Walls at Different Gaseous Fuel Ratios.
(a) Heat Input = 29 kW Runs 1,4,7,10,13
(b) Heat Input = 38 kW Runs 2,5,8,11,14
(c) Heat Input = 48 kW Runs 3,6,9,12,15

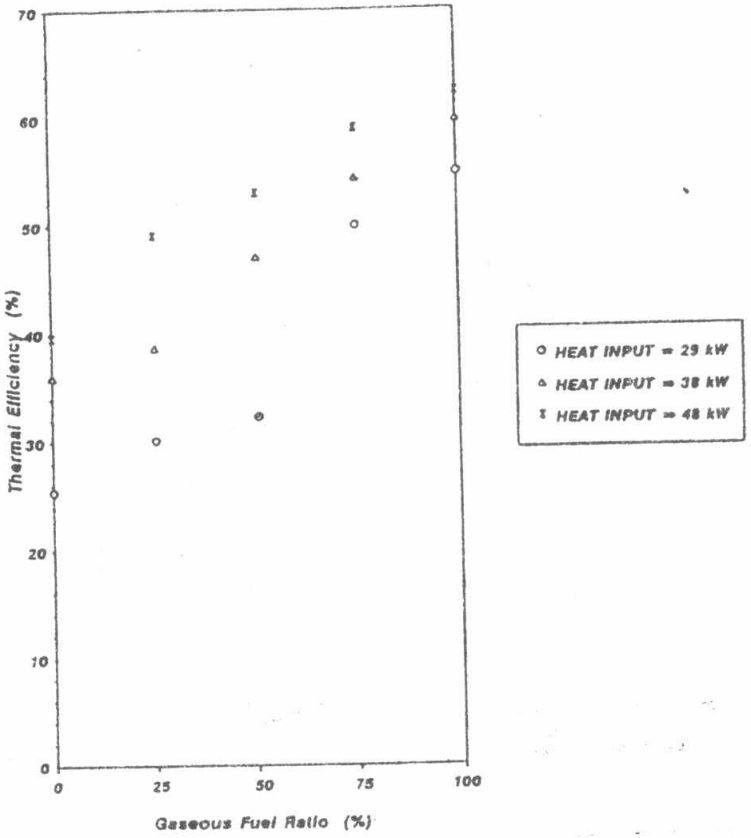

Fig. 11 *Comparison Between Thermal Efficiencies at Different Types of Fuel and at Different Heat Inputs.*

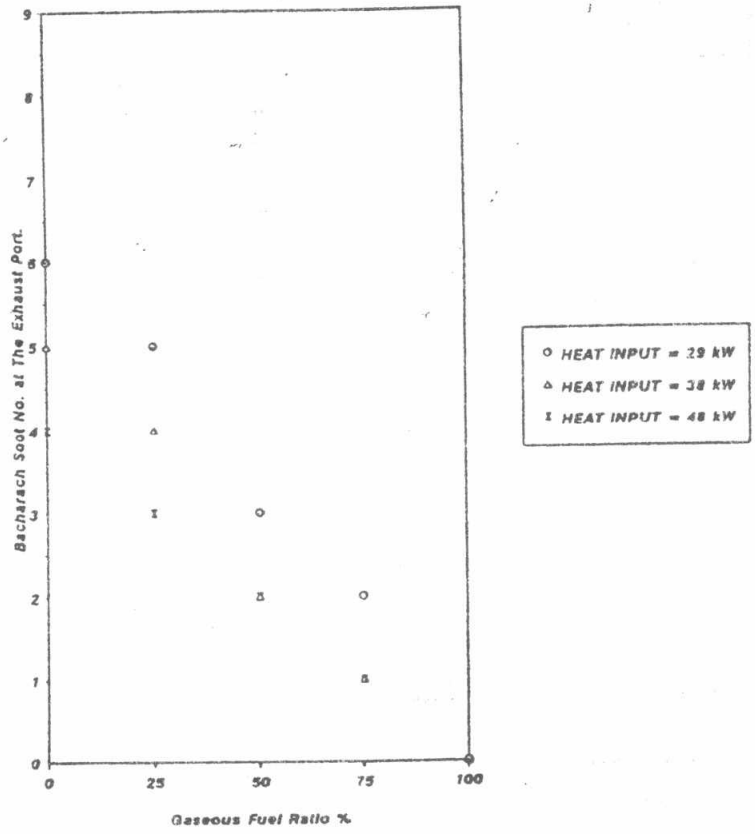

Fig. 12 *Comparison Between Soot Concentration at the Exhaust Port at Different Types of Fuel and at Different Heat Inputs*